The ISME Journal (2013) 7, 1803–1813

www.nature.com/ismej

ORIGINAL ARTICLE

Development of an ecophysiological model for *Diplosphaera colotermitum* TAV2, a termite hindgut Verrucomicrobium

Jantiya Isanapong[1,2], W Sealy Hambright[1], Austin G Willis[1], Atcha Boonmee[1,3], Stephen J Callister[4], Kristin E Burnum[4], Ljiljana Paša-Tolić[5], Carrie D Nicora[4], John T Wertz[6], Thomas M Schmidt[7] and Jorge LM Rodrigues[1]

[1]*Department of Biology, University of Texas–Arlington, Arlington, TX, USA;* [2]*Department of Earth and Environmental Sciences, University of Texas, Arlington, TX, USA;* [3]*Department of Microbiology, Faculty of Science, Khon Kaen University, Khon Kaen, Thailand;* [4]*Biological Sciences Division, Pacific Northwest National Laboratory, Richland, WA, USA;* [5]*Environmental and Molecular Sciences Laboratory, Pacific Northwest National Laboratory, Richland, WA, USA;* [6]*Department of Biology, Calvin College, Grand Rapids, MI, USA and* [7]*Department of Ecology and Evolutionary Biology and Department of Internal Medicine, University of Michigan, Ann Arbor, MI, USA*

Termite hindguts are populated by a dense and diverse community of microbial symbionts working in concert to transform lignocellulosic plant material and derived residues into acetate, to recycle and fix nitrogen, and to remove oxygen. Although much has been learned about the breadth of microbial diversity in the hindgut, the ecophysiological roles of its members is less understood. In this study, we present new information about the ecophysiology of microorganism *Diplosphaera colotermitum* strain TAV2, an autochthonous member of the *Reticulitermes flavipes* gut community. An integrated high-throughput approach was used to determine the transcriptomic and proteomic profiles of cells grown under hypoxia (2% O_2) or atmospheric (20% O_2) concentrations of oxygen. Our results revealed that genes and proteins associated with energy production and utilization, carbohydrate transport and metabolism, nitrogen fixation, and replication and recombination were upregulated under 2% O_2. The metabolic map developed for TAV2 indicates that this microorganism may be involved in biological nitrogen fixation, amino-acid production, hemicellulose degradation and consumption of O_2 in the termite hindgut. Variation of O_2 concentration explained 55.9% of the variance in proteomic profiles, suggesting an adaptive evolution of TAV2 to the hypoxic periphery of the hindgut. Our findings advance the current understanding of microaerophilic microorganisms in the termite gut and expand our understanding of the ecological roles for members of the phylum Verrucomicrobia.

The ISME Journal (2013) **7,** 1803–1813; doi:10.1038/ismej.2013.74; published online 9 May 2013
Subject Category: Integrated genomics and post-genomics approaches in microbial ecology
Keywords: termite; microaerophilic; *Verrucomicrobia*; xylan

Introduction

Termites have long been recognized for their ability to consume lignocellulosic plant material and soil (humus), converting it into substrates (primarily acetate) on which the termite depends for carbon and energy. These social insects are not only important for the global carbon cycling, but also for their biotechnological potential as efficient lignocellulose degraders (Brune, 1998). The success of termite feeding behavior is intimately associated with the presence of a diverse and abundant gut microbial community (Ohkuma and Brune, 2011). In the lower termite, *R. flavipes*, the complexity of symbiosis spans three domains of life: methane-producing Archaea, cellulolytic Eukarya (protozoa) and Bacteria—all acting cooperatively to degrade lignocellulose, fix/recycle nitrogen and remove oxygen, suggesting a division of metabolic activities among members of the community.

It has been long assumed that prokaryotic residents, in the hypoxic periphery of the termite gut, have the primary role of consuming O_2 and maintaining a steep radial gradient of this inwardly diffusing gas resulting in anoxia in the luminal portion of the gut (Brune *et al.*, 1995; Köhler *et al.*, 2012). However, this assumption has recently been challenged by the demonstration of a strong

Correspondence: JLM Rodrigues, Department of Biology, University of Texas–Arlington, Arlington, TX 76019, USA.
E-mail: Jorge@uta.edu
Received 20 December 2012; revised 16 March 2013; accepted 4 April 2013; published online 9 May 2013

correlation between the O_2 consumption rate of extracted guts and the number of protozoans per gut (Wertz and Breznak, 2007b), suggesting a more modest role for bacteria in this process—at least in those termites that possess (putatively 'strictly' anaerobic) cellulolytic protozoa in their hindguts. Although the relative importance of each group has yet to be resolved, it is reasonable to expect that microbial community members have multiple ecological functions, owing to their ubiquitous presence in different termite species.

Among the domain Bacteria, members of the phylum *Verrucomicrobia* have been consistently detected in molecular surveys of the 16S rRNA gene targeting the microbial community of various termite species (Hongoh *et al.*, 2003; Nakajima *et al.*, 2005; Berlanga *et al.*, 2011; Rosengaus *et al.*, 2011; Köhler *et al.*, 2012). Despite their ubiquity in higher and lower termite species, their functional role remains elusive. In an effort to understand the ecological functions of this microbial group, we previously isolated and characterized *Verrucomicrobia* strains from the gut of *R. flavipes*, including the new species *D. colotermitum* strain TAV2. We confirmed their autochthonous nature, estimated the population number and unveiled the genomic properties (Isanapong *et al.*, 2012, Wertz *et al.*, 2012), suggesting new ecological roles for *Verrucomicrobia* within the termite gut.

In this study, we investigate the microaerophilic nature of TAV2 and report on novel ecological functions. We employed comprehensive and integrative transcriptomic and proteomic approaches to: (1) identify genes and proteins being expressed in response to different O_2 concentrations; (2) develop an experimentally tested metabolic map for TAV2; and (3) establish the first ecophysiological model for an isolate of the phylum *Verrucomicrobia*.

Materials and methods

Culture conditions

D. colotermitum strain TAV2 (ATCC BAA-2264, DSMZ 25453) was grown in liquid R2A medium without agar (R2B) with a liquid-to-flask volume ratio of 40%. Four replicate cultures were incubated on an orbital shaker at 200 r.p.m inside a vinyl hypoxic chamber (Coy Laboratory Products, Glass Lake, MI, USA) fitted with an oxygen sensor and automated controller set for 2% or 20% O_2 concentration. These O_2 concentrations were selected because 60% of the termite hindgut is hypoxic (4% O_2 at the epithelial wall decreasing to anoxia approximately 100 μm inwards; Brune *et al.*, 1995), whereas 20% O_2 concentration approximates atmospheric O_2 concentrations (20.9% at 1 atm). When cells reached an optical density (OD_{600}) of 0.3 (approximately 8.7×10^7 cells per ml), 400 ml cultures were harvested by centrifugation (17 644 *g*) for 15 min at 4 °C. Cells were washed twice with ice-cold 50 mM phosphate-buffered saline (10 mM phosphate buffer (pH 7.0) and 130 mM NaCl), pellets were frozen immediately in liquid nitrogen and stored at −80 °C for further analysis. For the transcriptomic analysis, 5 ml of each culture was harvested by centrifugation for 5 min at 4 °C and immediately processed for RNA isolation.

Microarray design

The *D. colotermitum* microarray was designed to represent 4022 genes with coverage of three oligonucleotides per open reading frame. It contained 11 492 specific oligonucleotides (45–62 mer) replicated three times onto a glass slide (MYcroarray, Ann Arbor, MI, USA) and 166 oligonucleotides were introduced randomly throughout the slide as internal hybridization controls.

Microarray hybridization

Total RNA was extracted from cells grown under 2% and 20% O_2 conditions using the RiboPure bacterial RNA kit (Ambion, Austin, TX, USA), followed by DNase I treatment according to the manufacture's instructions. Transcripts were enriched with the MICROB*Express* bacterial mRNA enrichment kit (Ambion) and samples (100 ng) were amplified and converted to anti-sense RNA with the MessageAmp II anti-sense RNA amplification kit. Samples were ethanol precipitated and quality was assessed with the Bioanalyzer 2100 (Agilent Technologies, Santa Clara, CA, USA). Fluorescent labeling was performed with either Alexa Flour 555 or Alexa Flour 647 dyes, following instructions of the manufacturer (Invitrogen Inc., Carlsbad, CA, USA). Labeled samples were purified using the RNeasy kit (Qiagen Inc., Valencia, CA, USA), vacuum dried and stored at −20 °C until hybridization.

Slides were pre-hybridized with buffer containing 5× Saline-Sodium Phosphate EDTA (SSPE) (0.75 M NaCl, 0.05 M NaH_2PO_4, 0.005 M EDTA), 1% SDS and 1 mg ml^{-1} acetylated bovine serum albumin at 50 °C for 45 min and washed twice with 0.025× SSPE. Labeled samples (2.5 μg) were resuspended in 60 μl of 1× hybridization buffer (25% SSPE, 25% formamide, 0.05% Tween-20, 0.01 mg ml^{-1} bovine serum albumin) and transferred onto the slides. Single-slide rubber hybridization chambers were incubated in a 50 °C water bath for 16 h, followed by post-hybridization washes with 1× SSPE for 3 min and subsequently with 0.1× SSPE at room temperature for 1 min. A total of three technical replicates per biological replicate and respective dye swaps were used. Slides were scanned at a 30-μm resolution using the Genepix 4200 A scanner (Axon Instruments, Sunnyvale, CA, USA).

Transcriptomic data analysis

Signal intensities were normalized with the locally weighted scatterplot smoothing algorithm, log_2-transformed and filtered using a twofold change

cutoff (upper level set at 95% and lower level set at 10%) with the GeneSpring GX 11 software package (Agilent Technologies). Statistical analysis of differentially expressed genes was performed using the Student's *t*-test with subsequent correction with the Benjamini–Hochberg multiple-hypothesis adjustment (Cui and Churchill, 2003).

Protein extraction
Harvested *D. colotermitum* 2% O_2 and 20% O_2 growth samples were barocycled (Pressure Biosciences Inc., South Easton, MA, USA) from ambient (10 s) to 35 kpsi (20 s) for 10 times. RapiGestTM SF (Waters, Milford, MA, USA) and dithiothreitol (Sigma, St. Louis, MO, USA) were added to 0.1% and 5 mM concentrations, respectively. Samples were incubated at 60 °C for 30 min with gentle shaking. Proteins were digested using sequencing-grade modified porcine trypsin (Promega, Madison, WI, USA) and peptide concentration measured according to established protocols (Callister *et al.*, 2006).

Proteomic data analysis
Peptides were analyzed using the Accurate Mass and Time tag proteomics approach (Smith *et al.*, 2002) in combination with a reference peptide database empirically generated for *D. colotermitum*. For database generation, a pooled *D. colotermitum* sample was fractionated (50 fractions total) using strong cation exchange high-pressure liquid chromatography (HPLC). Each fraction was further separated by reverse phase HPLC coupled to a linear ion trap mass spectrometer (LTQ, ThermoFisher Scientific Corp., San Jose, CA, USA). Mass spectrometry (MS) instrument operating conditions and the HPLC separation method have previously been described (Sowell *et al.*, 2008). MS/MS spectra were analyzed using SEQUEST (Eng *et al.*, 1994) and the TAV2 genome (NCBI accession number ABEA00000000). Preliminary filtering of identified peptides was performed according to previously established criteria (Callister *et al.*, 2006).

Proteome abundance information was obtained by LTQ-Orbitrap MS analysis of peptides separated using reverse phase HPLC. Liquid chromatography (LC)-MS spectra were de-isotoped (Jaitly *et al.*, 2009), mass and elution time features identified, then matched (Monroe *et al.*, 2007) to peptides stored in the reference peptide database filtered to exclude non-tryptic peptides, and peptides having a PeptideProphet probability (Keller *et al.*, 2002) <0.50 (false discovery rate of less than 4%; Qian *et al.*, 2005). Matched peptides having a mass error <2 p.p.m. and normalized elution time error <0.06 were retained. Measured arbitrary abundance for a peptide was determined by integrating the area under each LC-MS peak for the detected feature matched to that peptide. Peptide abundances among technical replicates were combined, $\log_2$-transformed, normalized and converted to protein abundances with the ZRollup method implemented in DAnTE (Polpitiya *et al.*, 2008). Only proteins with two or more unique peptides were retained for ANOVA analysis (P-values <0.05 and q-values to control the false discovery rate below 0.04 in multiple testing; Storey 2002).

Metabolic reconstruction
A combined list of significantly expressed genes and detected proteins under both O_2 conditions was used for pathway prediction and metabolic overview of the strain TAV2 using the Oak Ridge National Laboratory annotation pipeline (http://genome.ornl.gov/microbial/verr/) and the Pathosystems Resource Integration Center genome viewer (http://patricbrc.vbi.vt.edu/).

Reverse transcription quantitative PCR (RT-qPCR)
Eight differentially expressed genes or proteins were selected for RT-qPCR analysis (Supplementary Table 1). Specific primers were designed with the Oligoanalyzer software (http://www.idtdna.com). Anti-sense RNA samples (5 μg) from the microarray analysis were reversed transcribed with the M-MuLV Taq RT-PCR kit (New England Biolabs, Ipswich, MA, USA). Complementary DNA (10 ng) was added to the SYBR Green master mix (Bio-Rad, Hercules, CA, USA) containing forward and reverse primers (150 nM each) and reactions were set according to manufacturer's instructions. Reactions were performed in triplicate for each biological replicate and results were normalized to the expression values of the housekeeping gene *gyrB* (β subunit of the DNA topoisomerase) to calculate fold induction values according to Livak and Schmittgen (2001). Statistical significance was calculated using the two-tailed Student's *t*-test.

Results

Confirmation of the microaerophilic phenotype of TAV2
Cells of *D. colotermitum* strain TAV2 were grown in liquid culture under controlled 2% or 20% O_2 concentrations. The growth rate during exponential phase for cells subjected to 2% O_2 was $0.0368\,h^{-1}$, whereas a growth rate of $0.0313\,h^{-1}$ was calculated for cells grown under 20% O_2 concentration ($P<0.001$). We determined that this difference in growth rates was sufficient to reduce the population doubling time by approximately 4 h for the 2% O_2 culture.

Transcriptome analysis
Microarray analysis allowed identification of 75 genes as differentially expressed ($P<0.05$), with an upregulation of 49 genes and a downregulation of 26

genes, when cells were grown under an atmosphere of 2% O_2 as opposed to 20% O_2. When differentially expressed genes were classified by functional categories based on clusters of orthologous groups (COGs) (Tatusov *et al.*, 1997), hypothetical genes or proteins of unknown function comprised 42.6% of the data set (Supplementary Table 1). Functional categories representing energy production and conversion, cell cycle control, replication and recombination, and cellular trafficking and secretion were present in the upregulated group for the 2% O_2 condition, whereas amino acid transport and metabolism and coenzyme transport were identified as downregulated functional groups.

Proteome analysis

A total of 36 109 peptides were identified in the LC-MS/MS analysis, with 18 044 and 18 065 peptides detected in samples derived from 2% O_2- and 20% O_2-grown cells, respectively. After data filtering to remove peptide and protein redundancies, 820 and 735 proteins were detected for each environmental condition, respectively. The above values account for 33% (2% O_2) and 30% (20% O_2), of the protein-coding genes identified in the high draft genome of *D. colotermitum*. Among identified proteins, 665 (74.7%) were detected in both culture conditions.

A total of 96 proteins were identified as upregulated ($P<0.05$), with 79 having higher spectral count measurements under 2% O_2, whereas 17 proteins were more abundant in cells growing under 20% O_2 concentration (Figure 1). Once assigned to functional categories, conserved hypothetical proteins or proteins encoded by genes previously classified as hypotheticals ranked as the largest group. The relative proportions of proteins classified in these two groups were 27.1% and 37.1% for 2% and 20% O_2, respectively. After removal of hypotheticals, the remaining proteins were placed in 22 COG categories in order to describe changes in cellular functions in response to O_2 (Figure 2). Eight COG categories had at least a twofold higher protein expression for cells grown under 2% O_2 in comparison to those grown under 20% O_2 conditions. These included: energy production and conversion (7.1%), carbohydrate transport and metabolism (5.8%), replication and recombination (5.8%). Only three categories had a two times higher protein expression under 20% O_2 condition: amino-acid transport and metabolism (8.4%), protein turnover and post-translational modifications (5.7%) and signal transduction mechanisms (2.9%). A principal component analysis of the proteomic results indicated that 72.34% of the variation could be explained by O_2 (55.9%), biological (9.67%) and technical (6.77%) replicates (Figure 3).

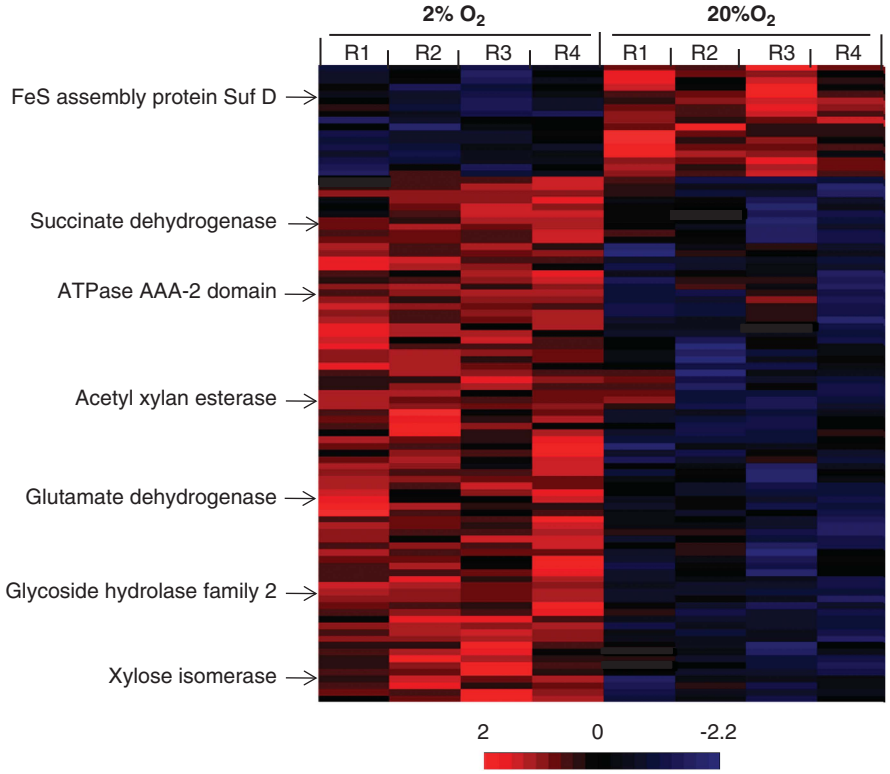

Figure 1 Heat map comparisons of calculated *Z*-scores for proteins differentially expressed by TAV2 cells grown under 2% or 20% O_2. Increasing intensity in the positive range (red) represents abundances that are greater than the mean abundance derived from both conditions relative to the standard deviation associated with the mean. A few enzymes discussed in the text are illustrated as indicated by the arrows.

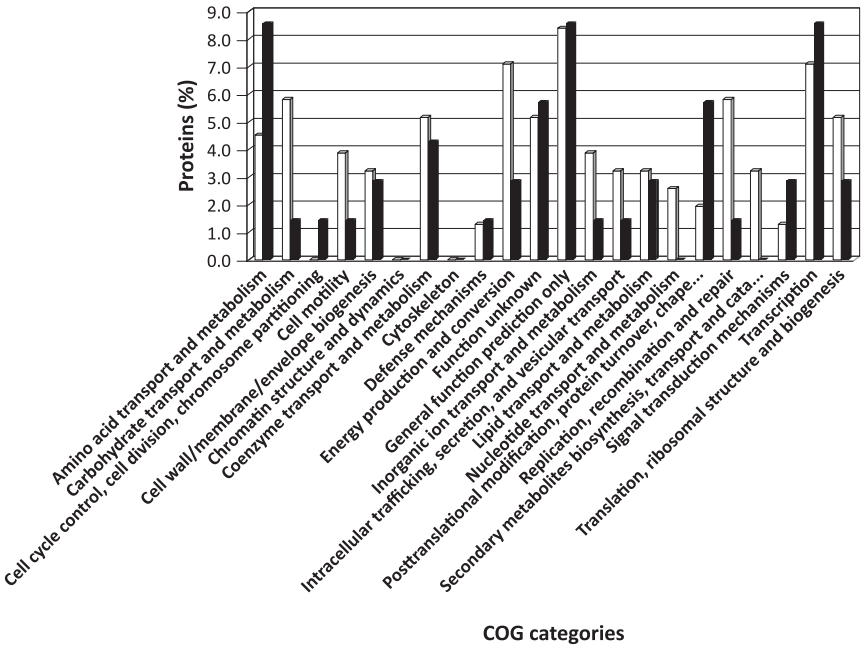

Figure 2 Relative proportions of unique proteins assigned to functional categories based on cluster of orthologous groups (COG). White bars represent proteins detected in cells grown under 2% O_2, whereas black bars represent proteins observed in cells grown under 20% O_2.

Transcriptomic and proteomic data comparison

We performed separate correlations for transcriptomic and proteomic data. The majority of the genes showed similar expression values in the two conditions tested ($R^2 = 0.7909$). The selection of differentially expressed genes modified the slope and lowered the coefficient of determination ($R^2 = 0.3748$). This is consistent with the larger number of genes that were upregulated under 2% O_2 in comparison to 20% O_2 (Supplementary Figure 1A). When the proteomic data were also examined in a similar manner, peptide abundances for proteins found in both conditions had a coefficient of determination of $R^2 = 0.8641$. The value was maintained approximately the same ($R^2 = 0.8543$) when only differentially detected proteins were selected for the calculation (Supplementary Figure 1B).

Next, we compared differentially expressed genes and proteins within the different COG categories. Clusters that had a large number of genes expressed also displayed a larger number of proteins being detected: energy production and conversion, carbohydrate transport and metabolism, and replication and recombination. An agreement between expressed transcripts and their corresponding proteins was only observed for a limited number of genes: ABC transporter, acetyl xylan esterase, ATP synthase, phosphofructokinase, ribosomal proteins, tetratricopeptide-repeat-containing protein, and a type II secretion system protein.

Metabolic reconstruction

We combined differentially expressed genes and proteins to construct a metabolic map for

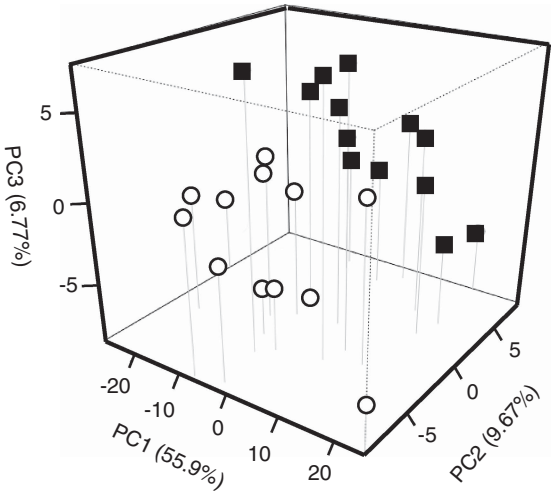

Figure 3 Principal component analysis of the proteome results for TAV2 cells grown under 2% or 20% O_2. Components were: (1) O_2 concentration, (2) biological replicate and (3) technical replicate. Open circles represent samples of cells grown under 2% O_2, whereas closed squares represent cells under 20% O_2.

D. colotermitum (Figure 4). Only enzymes assigned with an Enzyme Commission (EC) number were included in the reconstruction to provide an overall picture of TAV2 metabolism and determine the metabolic changes that occur in TAV2 at microoxic and atmospheric O_2 concentrations. The following functional categories were used for reconstruction:

Carbohydrate metabolism. Two major carbohydrate pathways were derived from the combined data: glycolysis and the pentose phosphate pathway (PPP). Eight out of the sixteen enzymes (50%)

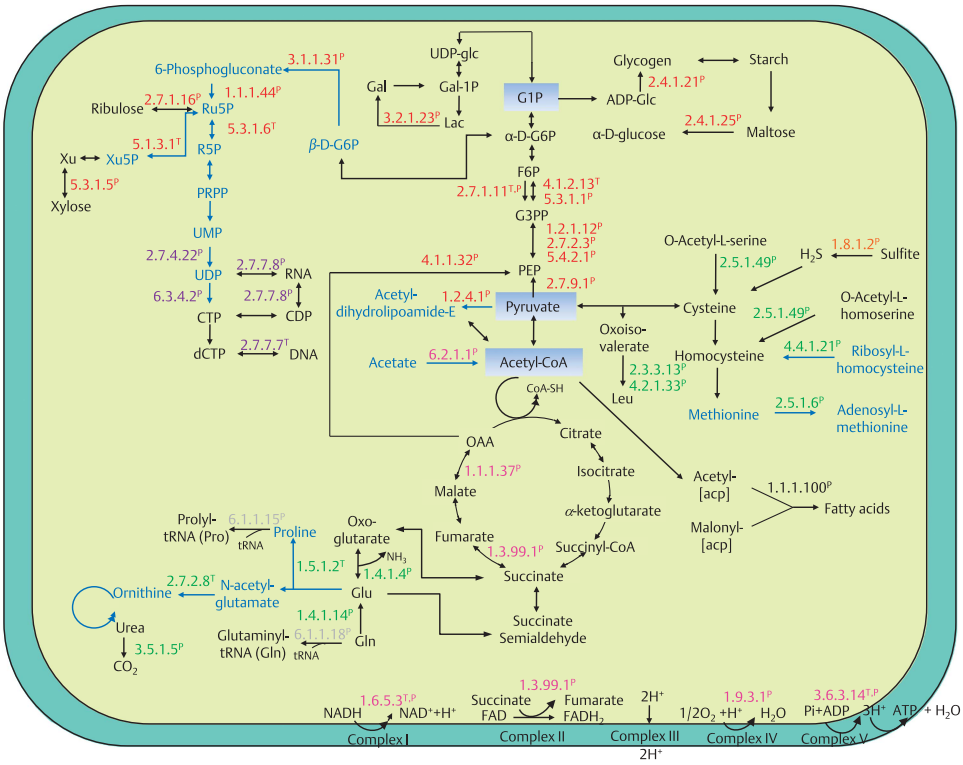

Figure 4 Metabolic map of *D. colotermitum* strain TAV2 constructed with selected differentially expressed genes and proteins. Proteins (P) and/or their mRNA transcripts (T) are classified into six major metabolic classes: carbohydrate metabolism (red), energy generation (pink), amino-acid biosynthesis (green), nucleotide metabolism (purple), fatty acid synthesis (black) and translation (gray). The enzyme sulfite reductase is shown in orange. Text marked in black represents upregulated pathways under 2% O_2, whereas text marked in blue represents downregulated pathways. acp, acyl carrier protein; ADP, adenosine diphosphate; ADP-glc, adenosine diphosphoglucose; CTP, cytidine triphosphate; CDP, cytidine diphosphate; dCTP, deoxycytidine triphosphate; Gal-1P, galactose-1-phosphate; Gal, galactose; G1P, glucose-1-phosphate; G6P, glucose-6-phosphate; G3PP, glyceraldehyde-3-phosphate; F6P, fructose-6-phosphate; FAD, flavin adenine dinucleotide (oxidized form); FADH, flavin adenine dincleotide (reduced form); Lac, lactose; Leu, leucine; Glu, glutamate; Gln, glutamine; NAD, nicotinamide adenine dinucleotide (oxidized form); NADH, nicotinamide adenine dinucleotide (reduced form); OAA, oxaloacetate; PEP, phosphoenolpyruvate; PRPP, phosphoribosyl pyrophosphate; Ru5P, ribulose 5-phosphate; R5P, ribose 5-phosphate; UDP-glc, uridine diphosphate glucose; UMP, uridine monophosphate; UDP, uridine diphosphate.

involved in glycolysis were upregulated under 2% O_2. Among these enzymes, a positive correspondence between transcriptomic and proteomic analyses was found for phosphofructokinase (EC: 2.7.1.11^{T,P}; superscript T and P denotes identification through transcriptome or proteome, respectively), the enzyme mediating the most important irreversible step from fructose 6-phosphate to fructose 1,6-bisphosphate. All enzymes associated with the PPP were downregulated under the same condition. It is noteworthy that the enzyme xylose isomerase (E.C.5.3.1.5^{P}) was upregulated. This enzyme is responsible for providing D-xylulose entering the PPP.

Malate dehydrogenase (EC:1.1.1.37^{P}) and succinate dehydrogenase (EC:1.3.99.1^{P}), two enzymes of the tricarboxylic acid cycle, were significantly upregulated under 2% O_2 concentration, whereas pyruvate dehydrogenase (acetyl-transferring; EC:1.2.4.1^{P}), the enzyme-mediating glucose catabolism, from glycolysis to the tricarboxylic acid (TCA) cycle was downregulated. The former two enzymes have been found to increase their activities under microaerobic growth (Pauling *et al.*, 2001), whereas the latter enzyme has its expression repressed by low levels of O_2. Interestingly, the enzyme pyruvate phosphate-dikinase (EC:2.7.9.1^{P}), an important enzyme in reversing glycolysis, was upregulated in cells maintained under microoxic conditions.

Upregulated genes and proteins were searched against the catalytic module of the carbohydrate-active enzyme database. We identified enzymes in four groups, as follows: glycosyl hydrolases (family 2 TIM barrel, 4-α-glucanotransferase (EC:2.4.1.25^{P})), carbohydrate esterases (acetyl xylan esterase (EC:3.1.1.72^{P})), glycosyl transferases (glycogen/starch synthase, ADP-glucose type (EC:2.4.1.21^{P})) and miscellaneous (xylose isomerase (EC:5.3.1.5^{P})).

Amino acid biosynthesis. Our metabolic reconstruction analysis indicated that strain TAV2 is capable of synthesizing amino acids essential to the termite host (leucine, lysine and tryptophan) and non-essential (alanine, glutamate, glutamine, cysteine and serine) under 2% O_2, whereas enzymes involved in the synthesis of proline, ornithine and methionine were downregulated. Noteworthy, both enzymes glutamate dehydrogenase (EC:1.4.1.4^{P}) and

glutamate synthase (EC:1.4.1.14^{P}), important for N metabolism, were upregulated; whereas the enzymes involved in the formation of proline, pyrroline-5-carboxylate reductase (EC:1.5.1.2^{T}) and ornithine, acetylglutamate kinase (EC:2.7.2.8^{T}), were downregulated. The presence of an enzyme involved in the biosynthesis of ornithine and the upregulated expression of the urease α-subunit domain protein (EC:3.5.1.5^{P}) denotes the importance for N recycling in the termite gut.

Energy transduction. TAV2 expressed several genes encoding for enzymes involved in the electron transport system and ATP synthesis. Enzymes such as NADH dehydrogenase (EC:1.6.5.3^{T,P}), succinate dehydrogenase (EC:1.3.99.1^{P}) and cytochrome c oxidase (EC:1.9.3.1^{P}) were significantly upregulated under microoxic conditions. A higher number of spectral counts was observed for the enzyme *cbb*$_3$ cytochrome oxidase for cells under 2% O_2 in comparison to those under 20% O_2. We observed a positive concurrence for the ATP synthase between proteomic and transcriptomic data, with both alpha (F_1) and beta (F_o) subunits of this large enzymatic complex (EC 3.6.3.14^{T,P}) significantly upregulated under 2% O_2 concentration, indicating that ATP formation is carried out through oxidative phosphorylation. Proteomic results showed a higher number of superoxide dismutase peptides for cells grown in 20% O_2 concentration, although this increase was slight and not statistically different from those obtained for samples grown under 2% O_2. This is consistent with the view that O_2 concentrations higher than those naturally found in the termite hindgut represent an oxidative stress for this microaerophile.

Nucleotide metabolism and post-translational modification. Genes and proteins involved in DNA replication, transcription and translation were highly expressed at 2% O_2. TAV2 showed a significant expression of enzymes (above three spectral counts) responsible for syntheses of pyrimidine bases, RNA and DNA. When combining proteomic and transcriptomic data, expressed genes and their detected proteins were observed for a subset of ribosomal proteins (L24^{P}, L9^{P}, S11^{P} and L15^{T}) and aminoacyl-tRNA transferases, such as glutaminyl-tRNA synthetase (EC:6.1.1.18^{P}), tryptophanyl-tRNA synthetase (EC:6.1.1.2^{P}) and lysyl-tRNA synthetase (EC:6.1.1.6^{T}). TAV2 expressed several proteins responsible for proofreading and degradation of mismatched DNA base pairs, such as the DNA mismatch repair protein MutS^{P}, and the exodeoxyribonuclease VII small subunit^{T}. Moreover, we observed the presence of proteins involved in gene regulation such as GreA/GreB family elongation factor^{P}, two component transcriptional regulator LuxR family^{P}, regulatory proteins LacI^{T} and GntR HTH^{T}, and translational proteins, such as the initiation factor 3^{P}, the protein that attaches the mRNA into 30S ribosome subunit, and the translation elongation factor G^{P}. The cytoplasmatic proteins in charge of protein folding, chaperonin GroEL^{P} and chaperonin cpn10^{P} were upregulated under 2% O_2 condition.

Secretion and transport systems. Our analysis showed that secretion and transport proteins had significantly higher spectral counts under 2% O_2 with significant expression of an ATP-binding cassette protein (ABC transporter), type II secretion system protein and tetratricopeptide-repeat-containing protein in both transcriptomic and proteomic analyses. The strain TAV2 expressed the enzyme SecA wing and scaffold^{P}, involved in the Sec translocase system. SecA is responsible for hydrolyzing ATP during protein export to the periplasm (Economou and Wickner, 1994). Under 2% O_2, TAV2 cells expressed solute-binding protein family 1^{P} and family 3^{P}. These carrier-mediated transport proteins help to increase the rate of solute uptake and accumulate solute inside the cells.

Validation of expressed genes through RT-qPCR
To confirm the transcriptomic results, induction values were calculated for eight selected genes using reverse transcription followed by quantitative PCR analysis. All upregulated genes selected for comparison were confirmed to be expressed at significantly higher levels (Supplementary Table 2). Owing to our particular interest in carbon metabolism, one acetyl xylan esterases ($P<0.05$) and three xylose isomerases (ObacDRAFT_3012, $P<0.01$; ObacDRAFT_1973 and ObacDRAFT_0419, $P<0.05$) that were not observed to be upregulated in our transcriptomic results, but showed $\geqslant$2-fold peptide change were included in this analysis. Upregulated expressions for all four genes were observed when measurements were carried out through RT-qPCR.

Discussion

The results of this study confirm the microaerophilic nature of strain TAV2 (Wertz *et al.*, 2012), with a higher growth rate observed for cells grown under 2% O_2 than those grown under 20% O_2. The long lag-phase shown for cells grown in 20% O_2 suggests the need of an acclimation period and the possibility of cells being under oxidative stress. Similarly, longer lag phases have been observed for the termite gut microaerophile *Stenoxybacter acetivorans* grown under increasing O_2 concentrations (Wertz and Breznak, 2007a). When TAV2 cells are maintained under 2% O_2, a condition associated with the physicochemical characteristics of the peripheral zone of the termite hindgut (30 mbar O_2; Brune *et al.*, 1995), genes associated with functional categories responsible for energy production and conversion, carbohydrate transport and metabolism, and

replication and recombination are upregulated as evidenced in both transcriptomic and proteomic data. It is noteworthy to observe that the COG category cell cycle control showed a divergent pattern between proteomic and transcriptomic approaches. We attribute this difference to the small number of genes (18 or 0.66% of the genome) belonging to cell cycle control in comparison to other categories. Refinements on gene identification and annotation methods will help to mitigate possible differences. In addition, several factors may explain transcriptome and proteome differences, such as post-translational modifications, half-lives of mRNA and proteins, and detection limits for both technologies (Zhang *et al.*, 2010).

TAV2 cells show signs of oxidative stress when grown under 20% O_2 condition. First, our proteomic approach detected the presence of peptides derived from superoxide dismutase. This result provides an explanation on how TAV2 manages reactive oxygen species and helps to conciliate our previous experimental work, in which the activity of superoxide dismutase was not observed (Wertz *et al.*, 2012). Second, TAV2 cells promote a shift in protein expression with a substantial increase of categories associated with amino-acid transport and metabolism, protein turnover and post-translational modifications, and signal transduction mechanisms. Specifically, proteins encoded by the *suf*C- and *suf*D-like genes in *Escherichia coli*, and predicted to be an ATPase and a complex-stabilizing protein (Nachin *et al.*, 2001, 2003), respectively, were highly abundant. These proteins are associated with the formation of [Fe-S] clusters and involved in repair during oxidative stress. Considering the importance of the initial microbial colonization of recently hatched termite larvae or frequent trophallactic transfers between individuals (Brune and Ohkuma, 2011), the presence of different mechanisms to cope with reactive oxygen species is an important feature for any termite microaerophile. Adaptations to O_2 toxicity might be a widespread attribute in the termite hindgut. Leadbetter and Breznak (1996) showed that methanogens, usually thought to be strict anaerobes, possess catalase activity. It is noteworthy that their isolates were *in situ* localized as present on or near the hindgut wall.

TAV2 cells employ the glycolytic pathway for processing carbohydrates to pyruvate and exert a tight control over the TCA cycle. The expression of pyruvate dehydrogenase, the enzyme responsible for providing acetyl-CoA to the TCA cycle, was downregulated under 2% O_2. Previously, Pauling *et al.* (2001) demonstrated that *Azorhizobium caulinodulans* cells exhibit a dramatic increase in $NADH/NAD^+$ ratio when cultures are shifted from aerobic to microaerobic conditions. It is possible that hypoxia in TAV2 also resulted in increase of NADH, a well-known inhibitor of the enzymes pyruvate dehydrogenase, citrate synthase, isocitrate dehydrogenase and α-ketoglutarate dehydrogenase (Barton, 2004), which slows down the overall activity of the TCA cycle. The adaptive consequence of a slow TCA cycle turnover remains to be investigated in depth for microaerophiles, but it suggests a controlled rate of substrate conversion. We hypothesize this metabolic design might be a consequence of the O_2 limitation, preventing NADH and $FADH_2$ from being readily oxidized. This is similar to the strategy used by fermentative bacteria operating a reductive TCA cycle (Ludwig, 2004). Although one might expect that the electron transport system and the ATP synthesis machinery may be affected as well, enzymes such as NADH dehydrogenase, cytochrome c oxidase and ATP synthase alpha (F_1) and beta (f_0) subunits were highly expressed under the low O_2 condition. This is consistent with previously observed increase in ATP formation with decreasing O_2 concentrations in other microaerophiles (Bergensen and Turner, 1975; Jackson and Dawes, 1976). Interestingly, Graber and Breznak (2004) observed a high molar ratio conversion for the termite spirochete *Treponema primitia* without substantial increase in biomass. The authors suggested that this mechanism would prevent overpopulation of the termite hindgut, destabilizing the symbiosis.

One of the well-known features of wood-feeding termites is that their diet is low in combined nitrogen (Potrikus and Breznak, 1981; Brune and Ohkuma, 2011). The TAV2 cell seems to be well adapted to its environment by carrying genes for biosynthesis of 20 of the most common amino acids plus ornithine. Our combined transcriptomic and proteomic data made possible for the identification of gene transcripts and proteins for biosynthesis of eight amino acids. This is a surprising finding considering that the growth medium was selected to elicit a broad metabolic response and contained yeast extract and casamino acids, albeit in low concentrations. The potential for biosynthesis and the expression of genes related to amino-acid formation have been shown for two protozoa endosymbionts (Hongoh *et al.*, 2008a, b) and two co-cultivated termite gut spirochete species (Rosenthal *et al.*, 2011). Previously, Sabree *et al.* (2012) proposed that the nutrient provisioning in termite–bacterial interaction was altered as the intracellular microorganism *Blattabacterium*, a symbiont in cockroaches, was replaced by hindgut protozoa and/or bacteria in almost all termite species. The presence of biosynthetic genes for all 20 common amino acids in the TAV2 genome and the subsequent expression of many of these genes suggest an array of possible interactions between the Verrucomicrobia population and its host as well as bacterial and protozoan members of the gut community.

Our proteomic results indicated the presence of specific peptides corresponding to the dinitrogenase reductase (NifH) only when cells were grown with 2% O_2, corroborating our previous findings for the

presence of nitrogen fixation genes (*nif*) and growth on N-free medium (Wertz *et al*., 2012). Finally, the expression of a urea-binding signal peptide protein and the α-subunit of urease may indicate a role for TAV2 in the recycling of uric acid excreted by the host. Previously, Potrikus and Breznak (1981) determined uricolysis to be a process mediated by gut bacteria occurring under anoxic conditions. The possibility that uric acid degradation occurs under microaerophilic conditions remains an interesting aspect of symbiosis, yet to be studied. Taken together, the above results imply that TAV2 can contribute to the nitrogen requirements of the termite. We remain cautious about establishing such a link based on the low *Verrucomicrobia* population size (1.2×10^3 cells) residing in the hindgut (Köhler *et al*., 2012; Wertz *et al*., 2012), but even a small contribution could be important in an N-limited ecosystem.

Lately, a renewed interest in the members of the phylum *Verrucomicrobia* has arisen because of their potential role in complex polysaccharide degradation (Flint *et al*., 2012; Martinez-Garcia *et al*., 2012) and importance in the biogeochemical cycling of carbon (Bergmann *et al*., 2011; Freitas *et al*., 2012). Although, we have yet to identify specific conditions allowing strain TAV2 to grow in xylan as a sole C source (Wertz *et al*., 2012), our integrated approach identified genes and proteins involved in lignocellulose degradation, specifically the enzymes acetylxylan esterase, xylan α-1,2-glucuronosidase and xylose isomerase, the later being responsible for converting xylose into xylulose, which enters the PPP (White, 2007). Because much of investigation in termite guts have targeted cellulose degradation through biochemical characterization of host celullases (Watanabe and Tokuda, 2010), gene expression of glycosyl hydrolases by protists (Todaka *et al*., 2007, 2010), and metagenomic (Warnecke *et al*., 2007) and proteomic (Burnum *et al*., 2011) approaches, the understanding of xylan hydrolysis remains virtually unexplored. Our results reveal an important and perhaps compartmentalized, ecological role for the TAV2 population on the debranching of xylan residues. Owing to the heteropolymeric structure of xylans, their degradation requires a coordinated action of a microorganism's transcriptional apparatus and a substantial metabolic investment on the production of many xylanolytic enzymes. We were able to identify different acetyl xylan esterases and xylose isomerases being expressed in TAV2 cells (Supplementary Table 2). It appears that the degradation of the xylans might be a wide-spread function among members of the phylum in different environments. Besides the strain TAV2, which belongs to the class *Opitutae,* soil isolates from classes *Verrucomicrobiae*, *Spartobacteria* and subdivision 3 were obtained with diluted medium containing xylan as a sole C source (Sangwan *et al*., 2005). Furthermore, experiments on single-cell genomics combined with fluorescently labeled xylan and laminarin in marine and fresh waters yielded *Verrucomicrobia* genomes particularly enriched in glycoside hydrolases (0.91% of total number of genes) in comparison to other sequenced bacterial genomes (0.2%) (Martinez-Garcia *et al*., 2012). Together, these independent results not only indicate an important ecological role in biopolymer recycling for the phylum, but also raise new questions on environmental conditions necessary for a coordinated response.

In this study, we asked whether O_2 was a relevant factor for the proteomic profile differences observed for strain TAV2. Approximately 55.9% of the variance is explained solely by changes in O_2 concentrations, suggesting a strong adaptive evolution of TAV2 within the wall-associated, oxygen-consuming termite gut community. Certainly, the identification of other environmental parameters and their combined effects on cell physiology will increase our understanding of the functional role of this species and other members of the phylum Verrucomicrobia.

A working model for D. colotermitum strain TAV2 in the R. flavipes hindgut

Our work provides the first integrated omics approach for understanding the ecological role of a member of the phylum *Verrucomicrobia*. We found that the TAV2 strain can contribute to the metabolism of the *R. flavipes* gut microbial community through biological N_2 fixation, amino-acid production, degradation of xylans and removal of free O_2. A conceptual model for the different functions carried out by the *D. colotermitum* strain TAV2 is proposed in Figure 5. Finally, our results underscore the importance of O_2 for whole-genome

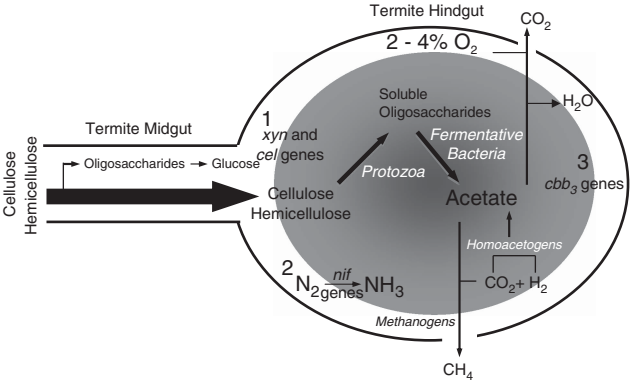

Figure 5 Model representation of possible functional roles for the *D. colotermitum* strain TAV2 in the hindgut of the termite *R. flavipes*. Strain TAV2 expressed genes and/or proteins associated with (1) hemicellulose degradation, (2) biological nitrogen fixation and (3) controlled oxygen consumption. Shaded area represents anoxic core and drawing is not to scale. Other important microbial groups are also represented in the hindgut ecosystem. For detailed morphological descriptions of microorganisms and the termite gut epithelium through transmission electron and scanning electron microscopy see Breznak and Pankratz (1977).

expression and, ultimately, the physiological state of a cell. Understanding the factors that regulate the microaerophilic physiology will broaden our view of an evolutionarily adapted group, sometimes mistakenly regarded as slow-growing aerobes.

Conflict of Interest

The authors declare no conflict of interest.

Acknowledgements

A portion of the research was performed using EMSL, a national scientific user facility sponsored by the Department of Energy's Office of Biological and Environmental Research and located at Pacific Northwest National Laboratory (EMSL 28690). We thank Maeli Melotto and John Breznak for critically reading this manuscript and providing valuable suggestions.

References

Barton LL. (2004). *Structural and Functional Relationships in Prokaryotes*. Springer: New York.

Bergensen FJ, Turner GL. (1975). Leghaemoglobin and the supply of O_2 to nitrogen-fixing root nodule bacteroids: presence of two oxidase systems and ATP production at low free O_2 concentration. *J Gen Microbiol* **91**: 345–354.

Bergmann GT, Bates ST, Eilers KG, Lauber CL, Caporaso JG, Walters WA *et al.* (2011). The under-recognized dominance of *Verrucomicrobia* in soil bacterial communities. *Soil Biol Biochem* **43**: 1450–1455.

Berlanga M, Pasteur BJ, Grandcolas P, Guerrero R. (2011). Comparison of the gut microbiota from soldier and worker castes of the termite *Reticulitermes grassei*. *Int Microbiol* **14**: 83–93.

Breznak JA, Pankratz HS. (1977). *In situ* morphology of the gut microbiota of wood-eating termites [*Reticulitermes flavipes* (Kollar) and *Coptotermes formosanus* Shiraki]. *Appl Environ Microbiol* **33**: 406–426.

Brune A, Emerson D, Breznak JA. (1995). The termite gut microflora as an oxygen sink: microelectrode determination of oxygen and pH gradients in lower and higher termites. *Appl Environ Microbiol* **61**: 2681–2687.

Brune A, Ohkuma M. (2011). Role of the termite gut microbiota in symbiotic digestion. In Bignell DE, Roisin Y, Lo N (eds). *Biology of Termites: a Modern Synthesis*. Springer: New York, NY, pp 439–475.

Brune A. (1998). Termite guts: the world's smallest bioreactors. *Trends Biotechnol* **16**: 16–21.

Burnum KE, Callister SJ, Nicora CD, Purvine SO, Hugenholtz P, Warnecke F *et al.* (2011). Proteome insights into the symbiotic relationship between a captive colony of *Nasutitermes corniger* and its hindgut microbiome. *ISME J* **5**: 161–164.

Callister SJ, Nicora CD, Zeng XH, Roh JH, Dominguez MA, Tavano CL *et al.* (2006). Comparison of aerobic and photosynthetic *Rhodobacter sphaeroides* 2.4.1 proteomes. *J Microbiol Methods* **67**: 424–436.

Cui X, Churchill GA. (2003). Statistical tests for differential expression in cDNA microarray experiments. *Genome Biol* **4**: 210.

Economou A, Wickner W. (1994). SecA promotes preprotein translocation by undergoing ATP-driven cycles of membrane insertion and deinsertion. *Cell* **78**: 835–843.

Eng JK, Mccomack AL, Yates JR. (1994). An approach to correlate tandem mass-spectral data of peptides with amino-acid-sequences in a protein database. *J Am Soc Mass Spectrom* **5**: 976–989.

Flint H, Scott K, Duncan S, Louis P, Forano E. (2012). Microbial degradation of complex carbohydrates in the gut. *Gut Microbes* **3**: 289–306.

Freitas S, Hatosy S, Fuhrman JA, Huse SM, Welsh DBM *et al.* (2012). Global distribution and diversity of marine *Verrucomicrobia*. *ISME J* **6**: 1499–1505.

Graber JR, Breznak JA. (2004). Physiology and nutrition of *Treponema primitia*, an H_2/CO_2-acetogenic spirochete from termite hindguts. *Appl Environ Microbiol* **70**: 1307–1314.

Hongoh Y, Ohkuma M, Kudo T. (2003). Molecular analysis of bacterial microbiota in the gut of the termite *Reticulitermes speratus* (Isoptera; Rhinotermitidae). *FEMS Microbiol Ecol* **44**: 231–242.

Hongoh Y, Sharma VK, Prakash T, Noda S, Taylor TD, Kudo T *et al.* (2008a). Complete genome of the uncultured Termite Group 1 bacteria in a single host protist cell. *Proc Natl Acad Sci USA* **105**: 5555–5560.

Hongoh Y, Sharma VK, Prakash T, Noda S, Toh H, Taylor TD *et al.* (2008b). Genome of an endoxymbiont compling N_2 fixation to cellulolysis within protist cells in the termite gut. *Science* **322**: 1108–1109.

Isanapong J, Goodwin L, Bruce D, Chen A, Detter C, Han J *et al.* (2012). High draft genome sequence of the *Opitutaceae* bacterium strain TAV1, a symbiont of the wood-feeding termite *Reticulitermes flavipes*. *J Bacteriol* **194**: 2744–2745.

Jackson FA, Dawes EA. (1976). Regulation of the tricarboxylic acid cycle and poly-β-hydroxybutyrate metabolism in *Azotobacter beijerinckii* grown under nitrogen or oxygen limitation. *J Gen Microbiol* **97**: 303–312.

Jaitly N, Mayampurath A, Littlefield K, Adkins JN, Anderson GA, Smith RD. (2009). Decon2LS: An open-source software package for automated processing and visualization of high resolution mass spectrometry data. *BMC Bioinformatics* **10**: 87.

Keller A, Nesvizhskii AI, Kolker E, Aebersold R. (2002). Empirical statistical model to estimate the accuracy of peptide identifications made by MS/MS and database search. *Anal Chem* **74**: 5383–5392.

Köhler T, Dietrich C, Scheffrahn RH, Brune A. (2012). High-resolution analysis of gut environment and bacterial microbiota reveals functional compartmentation of the gut in wood-feeding higher termites (*Nasutitermes* spp.). *Appl Environ Microbiol* **78**: 4691–4701.

Leadbetter JR, Breznak JA. (1996). Physiological ecology of *Methanobrevibacter cuticularis* sp. nov. and *Methanobrevibacter curvatus* sp. nov., isolated from the hindgut of the termite *Reticulitermes flavipes*. *Appl Environ Microbiol* **62**: 3620–3631.

Livak KJ, Schmittgen TD. (2001). Analysis of relative gene expression data using real-time quantitative PCR and the 2(-Delta Delta C(T)) method. *Methods* **25**: 402–408.

Ludwig RA. (2004). Microaerophilic bacteria transduce energy via oxidative metabolic gearing. *Res Microbiol* **155**: 61–70.

Martinez-Garcia M, Brazel DM, Swan BK, Arnosti C, Chain PSG, Reitenga KG *et al.* (2012). Capturing single cell genomes of active polysaccharide degraders: an unexpected contribution of *Verrucomicrobia*. *PLoS One* **4**: e353144.

Monroe ME, Tolic N, Jaitly N, Shaw JL, Adkins JN, Smith RD. (2007). VIPER: an advanced software package to support high-throughput LC-MS peptide identification. *Bioinformatics* **23**: 2021–2023.

Nachin L, Hassouni ME, Loiseau L, Expert D, Barras F. (2001). SoxR-dependent response to oxidative stress and virulence of *Erwinia chrysanthemi*: the key role of SufC, an orphan ABC ATPase. *Mol Microbiol* **39**: 960–972.

Nachin L, Loiseau L, Expert D, Barras F. (2003). SufC: an unorthodox cytoplasmic ABC/ATPase required for [Fe-S] biogenesis under oxidative stress. *EMBO J* **22**: 427–437.

Nakajima H, Hongh Y, Usami R, Kudo T, Ohkuma M. (2005). Spatial distribution of bacterial phylotypes in the gut of the termite *Reticulitermes speratus* and the bacterial community colonizing the gut epithelium. *FEMS Microb Ecol* **54**: 247–255.

Ohkuma M, Brune A. (2011). Diversity, structure, and evolution of the termite gut microbial community. In Bignell DE, Roisin Y, Lo N (eds). *Biology of Termites: a Modern Synthesis*. Springer: New York, NY, pp 413–438.

Pauling DC, Paris CA, Ludwig RA. (2001). *Azorhizobium caulinodans* pyruvate dehydrogenase activity is dispensable for aerobic but required for microaerobic growth. *Microbiology* **147**: 2233–2245.

Polpitiya AD, Qian WJ, Jaitly N, Petyuk VA, Adkins JN, Camp DG *et al.* (2008). DAnTE: a statistical tool for quantitative analysis of -omics data. *Bioinformatics* **24**: 1556–1558.

Potrikus CJ, Breznak JA. (1981). Gut bacteria recycle uric acid nitrogen in termites: a strategy for nutrient conservation. *Proc Natl Acad Sci USA* **78**: 4601–4605.

Qian WJ, Liu T, Monroe ME, Strittmatter EF, Jacobs JM, Kangas LJ *et al.* (2005). Probability-based evaluation of peptide and protein identifications from tandem mass spectrometry and SEQUEST analysis: The human proteome. *J Proteome Res* **4**: 53–62.

Rosengaus RB, Zecher CN, Shultheis KF, Brucker RM, Bordenstein SR. (2011). Disruption of the termite gut microbiota and its prolonged consequences for fitness. *Appl Environ Microbiol* **77**: 4303–4312.

Rosenthal AZ, Matson EG, Eldar A, Leadbetter JR. (2011). RNA-seq reveals comperative metabolic interactions between two termite-gut spirochete species in co-culture. *ISME J* **5**: 1133–1142.

Sabree ZL, Huang CY, Arakawa G, Tokuda G, Lo N, Watanabe H *et al.* (2012). Genome shrinkage and loss of nutrient-providing potential in the obligate symbiont of the primitive termite *Mastotermes darwiniensis*. *Appl Environ Microbiol* **78**: 204–210.

Sangwan P, Kovac S, Davis KER, Sait M, Janssen PH. (2005). Detection and cultivation of soil *Verrucomicrobia*. *Appl Environ Microbiol* **71**: 8402–8410.

Smith RD, Anderson GA, Lipton MS, Pasa-Tolic L, Shen YF, Conrads TP *et al.* (2002). An accurate mass tag strategy for quantitative and high-throughput proteome measurements. *Proteomics* **2**: 513–523.

Sowell SM, Norbeck AD, Lipton MS, Nicora CD, Callister SJ, Smith RD *et al.* (2008). Proteomic analysis of stationary phase in the marine bacterium 'Candidatus *Pelagibacter ubique*'. *Appl Environ Microbiol* **74**: 4091–4100.

Storey D. (2002). A direct approach to false discovery rates. *J Royal Stat Soc S B* **64**: 479–498.

Tatusov RL, Koonin EV, Lipman DJ. (1997). A genomic perspective on protein families. *Science* **278**: 631–637.

Todaka N, Inoue T, Saita K, Ohkuma M, Nalepa CA, Lenz M *et al.* (2010). Phylogenetic analysis of cellulolytic enzyme genes from representative lineages of termites and a related cockroach. *PLoS One* **5**: e8636.

Todaka N, Moriya S, Saita K, Hondo T, Kiuchi I, Takasu H *et al.* (2007). Environmental cDNA analysis of the genes involved in lignocellulose digestion in the symbiotic protist community of *Reticulitermes speratus*. *FEMS Microbiol Ecol* **59**: 592–599.

Warnecke F, Luginbuhl P, Ivanova N, Ghassemian M, Richardson TH, Stege JT *et al.* (2007). Metagenomic and functional analysis of hindgut microbiota of a wood-feeding higher termite. *Nature* **450**: 560–570.

Watanabe H, Tokuda G. (2010). Cellulolytic systems in insects. *Annu Rev Entomol* **55**: 609–632.

Wertz JT, Breznak JA. (2007a). *Stenoxybacter acetivorans* gen. nov., an acetate-oxidizing obligate microaerophile among diverse O_2-consuming bacteria from termite guts. *Appl Environ Microbiol* **73**: 6819–6828.

Wertz JT, Breznak JA. (2007b). Physiological ecology of *Stenoxybacter acetivorans*, an obligate microaerophile in termite guts. *Appl Environ Microbiol* **73**: 6829–6841.

Wertz JT, Kim E, Breznak JA, Schmidt TM, Rodrigues JLM. (2012). Genomic and physiological characterization of the *Verrucomicrobia* isolate *Diplosphaera colotermitum* gen. nov., sp. nov., reveals microaerophily and nitrogen fixation genes. *Appl Environ Microbiol* **78**: 1544–1555.

White D. (2007). *The Physiology and Biochemistry of Prokaryotes*. Oxford University Press: New York.

Zhang W, Li F, Nei L. (2010). Integrating multiple 'omics' analysis for microbial biology: application and methodologies. *Microbiology* **156**(Pt 2): 287–301.

Supplementary Information accompanies this paper on The ISME Journal website (http://www.nature.com/ismej)